Report 11340
11 November 1998

Integrated Advanced Microwave Sounding Unit-A (AMSU-A)

Engineering Test Report

AMSU EOS A1 Thermal Balance Test Correlation

Contract No. NAS 5-32314
CDRL 207

Submitted to:

National Aeronautics and Space Administration
Goddard Space Flight Center
Greenbelt, Maryland 20771

Submitted by:

Aerojet
1100 West Hollyvale Street
Azusa, California 91702

GENCORP
AEROJET

Azusa Operations

INTEROFFICE MEMO

TO:	RV Hauerwaas	DATE:11 Nov. 98 Bldg 170:8421:X1232
FROM:	RJ Krylo	RJK:**98#813**
SUBJECT:	AMSU EOS A1 Thermal Balance Test Correlation	
COPIES TO:	J Alvarez, J Jansen, R Kapper, F Kerwin, L Paliwoda, P Patel, R Platt, C Neves, J Misselhorn, L Rempt, T Lawson	

References 1) AE-26151/11, "Thermal Balance Test Procedure For EOS/AMSU-A System", dated 27 August 1998

2) AE-26151/9A, "Test Procedure, Thermal Cycling For the EOS AMSU-A ", dated 6 July 1998

Purpose Publish the results of the EOS AMSU-A1 thermal balance test.

Summary Based on correlations to three steady state test points, 11 changes are required of the EOS A1 thermal models-

1) Reduce the electrical power from 76.6W to 71.4W.
2) Increase the MLI blanket ε^* connections from 0.02 to 0.05.
3) Revise the rotating reflector stripes by enlarging the feedhorn shroud and feedhorn panel and reducing the snout and reflector shroud.
4) Remove the 10% reduction in internal radiation from the K correlation.
5) Remove the 5% reduction in external radiation from the K correlation.
6) Increase the radiator and IR plate emissivities by 5%.
7) Increase the DC/DC converter-to-panel conduction by 20%.
8) Increase the radiator panel conduction beneath the DC/DC convertor by 2 times to account for the convertor housing.
9) Increase the feedhorn-to-shroud and shroud-to-panel conduction by 50%.
10) Increase the RF shelf-to-wall conduction by 25%.
11) Add the external cables.

These changes produce a temperature correlation that ranges from 3.4°C warmer than the measurements to 3.4°C cooler. On the average, the predictions are 0.3°C warmer than the measurements.

Action Thermal engineering will incorporate these changes into the EOS-A1 "free flyer" thermal math models and make new orbital temperature predictions.

Discussion Thermal balance testing consists of predicting the instrument temperatures in the test configuration, measuring the instrument temperatures at several steady state conditions, and reconciling the differences between the predicted and measured temperatures.

Predictions come from thermal models specially developed for the thermal balance test. Figures 1-3 show the model geometry. The models consist of the AMSU-A1 "free flyer" surrounded by the calibration targets, target supports, IR plates, and mounting plates.

Temperature measurements come from the flight sensors and thermocouples added for the test. References 1 and 2 show the thermocouples on the test fixture and the thermocouples added to the outside of the AMSU instrument. All of the IR plates, the instrument mounting plate, and fixture baseplate have thermocouples. The temperature measurements from the calibration targets, IR plates, and baseplates become boundary temperatures for the thermal model.

IR Plates 5, 6, and 7, shown on figure 2, are new for this test. They fill open areas of the test fixture with surfaces of known temperature. Ideally, the surroundings would be the inside of a black temperature controlled shroud. The A1 test chamber, however, is too small for a shroud. Instead, a black tedlar blanket covers the fixture. IR plates 5, 6, and 7 reduce the uncertainty of viewing this otherwise unmonitored blanket.

An important feature of this test is acquiring data at near steady state. Steady state is important because it eliminates the effects of thermal capacitance, making the correlation effort less complex. Steady state is appropriate for AMSU because orbital transients are mild.

Thermal stability is determined by monitoring the slowest responding components, the warm loads, during transitions and comparing them to projected steady state temperatures. Projected steady state temperatures come from fitting the transition temperatures to equation 8002, a simple exponential decay, from Table Curve 2D. Temperature stability is declared when the temperatures of the warm loads are within 1C of the projected steady states.

Three cases provide data for the test. The first is a hot case with warm IR plates, warm spacecraft plate, and warm variable calibration targets. The second is a cold case with cold IR plates, cold spacecraft plate, and cold variable calibration targets. The third is a cold case with cold IR plates, cold spacecraft plate, and ambient temperature variable and fixed calibration targets. Case 3 nearly eliminates heat transfer to the calibration targets for a simpler correlation.

The raw data for thermal balance, as well as thermal vacuum cycling, is stored in Shop Order 598513 under synthetic part number 1356008-1-TVA.

Two kinds of changes lead to thermal model correlation, global and local. Global changes produce an overall increase or decrease in predicted temperatures while local changes usually cool an individual component or hot spot. The global changes are:

•Reduce the power from 76.6W to 71.4W, based on the measured quiet bus power and voltage. Do this by simply reducing all power dissipations by 6.8%.
•Increase the MLI blanket e star from .02 to .05 allowing more heat to leak through the blankets.
•Revise the rotating reflector stripes to reject more heat. Figure 3 shows the modelling technique for the reflectors. Multiple cylindrical stripes, assigned to the reflector shroud, mirror, feedhorn wall and feedhorn, give a stationary view through the otherwise rotating reflector. Increasing the feedhorn and feedhorn wall stripe areas increases the radiation coupling and hence heat rejection to the external calibration targets.
•Remove the 10% reduction in internal radiation from the K correlation, providing higher coupling from the components to the walls.
•Remove the 5% external emissivity reduction from the K correlation, providing increased coupling to the IR plates.
•Increase the emissivities of the radiators and IR plates by 5%.

The local changes are:

•Increase the DC/DC converter-to-panel conduction by 20%. This modifies the path from the thermal sensor location on the converter housing to the bolted interface at the radiatior panel.
•Increase the radiator panel conduction beneath the converter to account for the convertor housing. Neither the metal of the housing, which runs in parallel with the radiator panel, nor the heat distribution of the mounting feet are in the thermal model. These features effectively raise the conduction of the radiator panel.
•Increase both feedhorn-to-feedhorn shroud and feedhorn shroud-to-panel conductances by 50%.
•Increase the RF shelf-to-wall conduction by 25% for both shelves.
•Add the external cables. The cables are uninsulated in the test and are radiatively coupled to IR plates 1, 2, and 3.

The combined result is an average error of -0.26°C, and maximum errors of +3.4°C and -3.4°C. Tables I-III show the results.

Table I. Hot Thermal Balance Correlation for Oct. 2, 1998

Predicted °C	Measured °C	Error °C	Node	Description
26.3	24.4	-1.9	259	RT1, WARMLOAD A1-1
22.6	21.8	-0.8	159	RT6, WARMLOAD A1-2
33.4	32.8	-0.6	241	RT11, TOP OF DRO CHANNEL 7
32.9	35.5	2.5	418	RT12, TOP OF DRO CHANNEL 8
34.9	32.8	-2.2	242	RT13, TOP OF DRO CHANNEL 15
31.0	29.3	-1.7	244	RT14, TOP OF PLO
37.9	36.9	-1.0	243	RT15, TOP OF PLO
33.9	33.5	-0.4	411	RT17, TOP OF MIXER IF CH.3
33.4	33.4	0.0	412	RT18, TOP OF MIXER IF CH.4
32.3	32.6	0.3	413	RT19, TOP OF MIXER IF CH.5
32.6	31.9	-0.8	223	RT20, TOP OF MIXER IF CH.6
33.3	31.8	-1.5	226	RT21, TOP OF MIXER IF CH.7
33.5	33.4	-0.1	414	RT22, TOP OF MIXER IF CH.8
32.0	30.4	-1.6	225	RT23, TOP OF MIXER IF CH.9/14
34.1	34.4	0.3	224	RT24, TOP OF MIXER IF CH.15
34.5	32.5	-2.0	239	RT25, SIDE OF IF AMP CH.11/14
34.7	32.5	-2.2	234	RT26, SIDE OF IF AMP CH.9
35.1	32.9	-2.2	233	RT27, SIDE OF IF AMP CH.10
29.7	31.5	1.8	235	RT28, SIDE OF IF AMP CH.11
29.7	31.3	1.6	236	RT29, SIDE OF IF AMP CH.12
29.6	30.8	1.1	237	RT30, SIDE OF IF AMP CH.13
29.7	31.9	2.3	238	RT31, SIDE OF IF AMP CH.14
34.5	32.7	-1.8	280	RT32, DC/DC CONVERTER
32.0	31.9	-0.1	60	RT33, UPPER RF SHELF
33.3	30.7	-2.5	206	RT34, LOWER RF SHELF
32.2	31.5	-0.7	279	RT35, DETECTOR/PREAMP
26.1	24.1	-2.0	175	RT36, SCAN MOTOR A1-1
21.6	22.2	0.6	65	RT37, SCAN MOTOR A1-2
28.0	25.6	-2.5	221	RT38, FEEDHORN A1-1
24.2	23.4	-0.9	401	RT39, FEEDHORN A1-2
32.2	30.9	-1.3	222	RT40, RF MUX A1-1
29.2	32.2	2.9	402	RT41, RF MUX A1-2
33.0	35.7	2.7	415	RT42, TOP OF DRO CHANNEL 3
32.7	35.9	3.1	416	RT43, TOP OF DRO CHANNEL 4
32.2	34.0	1.8	417	RT44, TOP OF DRO CHANNEL 5
31.9	31.7	-0.1	240	RT45, TOP OF DRO CHANNEL 6
14.1	13.8	-0.3	3	M1, TOP PANEL
19.9	20.1	0.2	29	M2, RIGHT SIDE UPPER PANEL
17.9	19.5	1.6	313	M3, RIGHT LOWER SIDE WALL, TOP
19.8	20.7	0.9	316	M4, RIGHT LOWER SIDE WALL, BOTTOM
24.5	24.6	0.1	38	M5, LEFT SIDE PANEL, TOP
27.0	25.4	-1.6	33	M6, UPPER AFT PANEL
22.9	24.3	1.4	304	M7, LOWER AFT WALL
27.8	27.0	-0.8	336	M8, LEFT SIDE PANEL, BOTTOM
26.7	25.4	-1.3	182	M9, BASEPLATE
26.1	25.6	-0.5	184	M10, BASEPLATE

Table II. Cold Thermal Balance Correlation for Oct.4, 1998

Predicted °C	Measured °C	Error °C	Node	Description
-3.1	-5.2	-2.1	259	RT1, WARMLOAD A1-1
-6.2	-7.9	-1.7	159	RT6, WARMLOAD A1-2
6.0	4.8	-1.2	241	RT11, TOP OF DRO CHANNEL 7
5.5	6.5	1.0	418	RT12, TOP OF DRO CHANNEL 8
7.6	4.7	-2.9	242	RT13, TOP OF DRO CHANNEL 15
3.8	1.5	-2.3	244	RT14, TOP OF PLO
11.0	9.3	-1.7	243	RT15, TOP OF PLO
6.3	5.0	-1.3	411	RT17, TOP OF MIXER IF CH.3
5.9	5.0	-0.9	412	RT18, TOP OF MIXER IF CH.4
4.8	4.3	-0.5	413	RT19, TOP OF MIXER IF CH.5
5.0	3.7	-1.3	223	RT20, TOP OF MIXER IF CH.6
5.6	3.8	-1.8	226	RT21, TOP OF MIXER IF CH.7
6.0	4.8	-1.2	414	RT22, TOP OF MIXER IF CH.8
4.4	2.4	-2.0	225	RT23, TOP OF MIXER IF CH.9/14
6.6	6.5	-0.1	224	RT24, TOP OF MIXER IF CH.15
7.5	4.8	-2.7	239	RT25, SIDE OF IF AMP CH.11/14
7.8	5.0	-2.7	234	RT26, SIDE OF IF AMP CH.9
8.1	5.0	-3.1	233	RT27, SIDE OF IF AMP CH.10
2.7	3.7	1.1	235	RT28, SIDE OF IF AMP CH.11
2.7	3.5	0.8	236	RT29, SIDE OF IF AMP CH.12
2.6	3.1	0.5	237	RT30, SIDE OF IF AMP CH.13
2.7	4.3	1.6	238	RT31, SIDE OF IF AMP CH.14
7.9	5.5	-2.4	280	RT32, DC/DC CONVERTER
4.5	3.5	-1.0	60	RT33, UPPER RF SHELF
5.9	2.9	-3.1	206	RT34, LOWER RF SHELF
2.9	3.4	0.5	279	RT35, DETECTOR/PREAMP
-4.3	-6.6	-2.3	175	RT36, SCAN MOTOR A1-1
-8.9	-8.8	0.0	65	RT37, SCAN MOTOR A1-2
-1.3	-4.7	-3.4	221	RT38, FEEDHORN A1-1
-5.7	-6.6	-0.9	401	RT39, FEEDHORN A1-2
4.3	2.9	-1.5	222	RT40, RF MUX A1-1
0.9	3.5	2.6	402	RT41, RF MUX A1-2
5.5	6.7	1.2	415	RT42, TOP OF DRO CHANNEL 3
5.2	6.8	1.6	416	RT43, TOP OF DRO CHANNEL 4
4.7	5.7	1.0	417	RT44, TOP OF DRO CHANNEL 5
3.8	2.9	-0.9	240	RT45, TOP OF DRO CHANNEL 6
-13.4	-14.3	-0.9	3	M1, TOP PANEL
-7.3	-7.6	-0.3	29	M2, RIGHT SIDE UPPER PANEL
-9.2	-8.2	1.0	313	M3, RIGHT LOWER SIDE WALL, TOP
-7.0	-6.2	0.8	316	M4, RIGHT LOWER SIDE WALL, BOTTOM
-3.7	-3.7	0.0	38	M5, LEFT SIDE PANEL, TOP
0.1	-2.1	-2.2	33	M6, UPPER AFT PANEL
-4.4	-3.0	1.4	304	M7, LOWER AFT WALL
-0.2	-1.3	-1.1	336	M8, LEFT SIDE PANEL, BOTTOM
-1.0	-2.4	-1.4	182	M9, BASEPLATE
-2.4	-2.9	-0.5	184	M10, BASEPLATE

Table III. Ambient Target Thermal Balance Correlation for Oct. 14, 1998

Predicted °C	Measured °C	Error °C	Node	Description
4.0	4.5	0.4	259	RT1, WARMLOAD A1-1
2.1	1.6	-0.4	159	RT6, WARMLOAD A1-2
12.7	13.1	0.4	241	RT11, TOP OF DRO CHANNEL 7
12.9	14.2	1.3	418	RT12, TOP OF DRO CHANNEL 8
13.0	11.3	-1.7	242	RT13, TOP OF DRO CHANNEL 15
15.4	15.9	0.5	244	RT14, TOP OF PLO
9.9	8.4	-1.5	243	RT15, TOP OF PLO
13.8	12.4	-1.5	411	RT17, TOP OF MIXER IF CH.3
13.3	12.3	-1.0	412	RT18, TOP OF MIXER IF CH.4
12.2	11.5	-0.7	413	RT19, TOP OF MIXER IF CH.5
11.3	11.7	0.4	223	RT20, TOP OF MIXER IF CH.6
11.9	11.4	-0.4	226	RT21, TOP OF MIXER IF CH.7
13.5	12.3	-1.2	414	RT22, TOP OF MIXER IF CH.8
10.6	10.2	-0.4	225	RT23, TOP OF MIXER IF CH.9/14
12.5	14.0	1.5	224	RT24, TOP OF MIXER IF CH.15
12.1	11.3	-0.8	239	RT25, SIDE OF IF AMP CH.11/14
12.4	11.5	-0.9	234	RT26, SIDE OF IF AMP CH.9
12.8	11.5	-1.3	233	RT27, SIDE OF IF AMP CH.10
9.0	11.4	2.4	235	RT28, SIDE OF IF AMP CH.11
9.1	11.2	2.2	236	RT29, SIDE OF IF AMP CH.12
9.0	10.8	1.8	237	RT30, SIDE OF IF AMP CH.13
9.0	11.9	2.9	238	RT31, SIDE OF IF AMP CH.14
13.4	11.6	-1.8	280	RT32, DC/DC CONVERTER
12.0	10.7	-1.2	60	RT33, UPPER RF SHELF
12.0	10.7	-1.2	206	RT34, LOWER RF SHELF
10.5	11.8	1.3	279	RT35, DETECTOR/PREAMP
4.4	4.4	0.0	175	RT36, SCAN MOTOR A1-1
2.1	2.2	0.1	65	RT37, SCAN MOTOR A1-2
7.2	5.5	-1.7	221	RT38, FEEDHORN A1-1
4.5	2.0	-2.5	401	RT39, FEEDHORN A1-2
10.8	10.5	-0.3	222	RT40, RF MUX A1-1
9.3	11.0	1.7	402	RT41, RF MUX A1-2
13.0	14.4	1.4	415	RT42, TOP OF DRO CHANNEL 3
12.7	14.5	1.8	416	RT43, TOP OF DRO CHANNEL 4
12.2	12.9	0.8	417	RT44, TOP OF DRO CHANNEL 5
10.6	11.4	0.8	240	RT45, TOP OF DRO CHANNEL 6
-7.7	-8.6	-0.9	3	M1, TOP PANEL
-1.7	-1.8	-0.1	29	M2, RIGHT SIDE UPPER PANEL
-3.0	-0.5	2.5	313	M3, RIGHT LOWER SIDE WALL, TOP
-2.3	0.1	2.4	316	M4, RIGHT LOWER SIDE WALL, BOTTOM
3.5	3.8	0.3	38	M5, LEFT SIDE PANEL, TOP
5.6	4.1	-1.5	33	M6, UPPER AFT PANEL
-0.7	2.7	3.4	304	M7, LOWER AFT WALL
5.8	6.4	0.6	336	M8, LEFT SIDE PANEL, BOTTOM
3.7	4.1	0.4	182	M9, BASEPLATE
3.5	5.2	1.7	184	M10, BASEPLATE

Tables I-III contain the temperatures measured on the instrument. Table IV contains the measurements made on the test fixture.

Table IV. Boundary Temperatures

Node	Description	Temp., °C Oct. 2	Temp., °C Oct. 4	Temp., °C Oct. 14
9101	IR PLATE #1	-18.7	-60.5	-59.9
9102	IR PLATE #2	-19.3	-60.1	-60.1
9103	IR PLATE #3	-19.7	-60.8	-59.5
9104	IR PLATE #4	-50.1	-90.3	-90.6
9105	IR PLATE #5	12.0	-36.8	-8.2
9106	IR PLATE #6	4.1	-34.6	-6.0
9107	IR PLATE #7	-6.2	-45.8	-12.1
9231	A1-2 FIXED TARGET	-189.4	-189.4	5.0
9431	A1-2 VARIABLE TARGET	56.8	-189.4	5.0
9631	A1-1 FIXED TARGET	-189.4	-189.4	5.2
9831	A1-1 VARIABLE TARGET	56.8	-189.4	4.9
9911	BASEPLATE	12.0	-26.9	4.7
998	EOS SPACECRAFT PLATE	30.3	0.2	0.0

The measure of success for a thermal balance test is errors of 3°C or less. This correlation produces errors of 3.4°C or less which substantially meets the goal.

Conclusions The 11 changes presented here correlate the EOS AMSU-A1 thermal models to the thermal balance test data. These changes will be applied to the orbital models and new predictions made.

Robert Krylo
Thermal Engineer

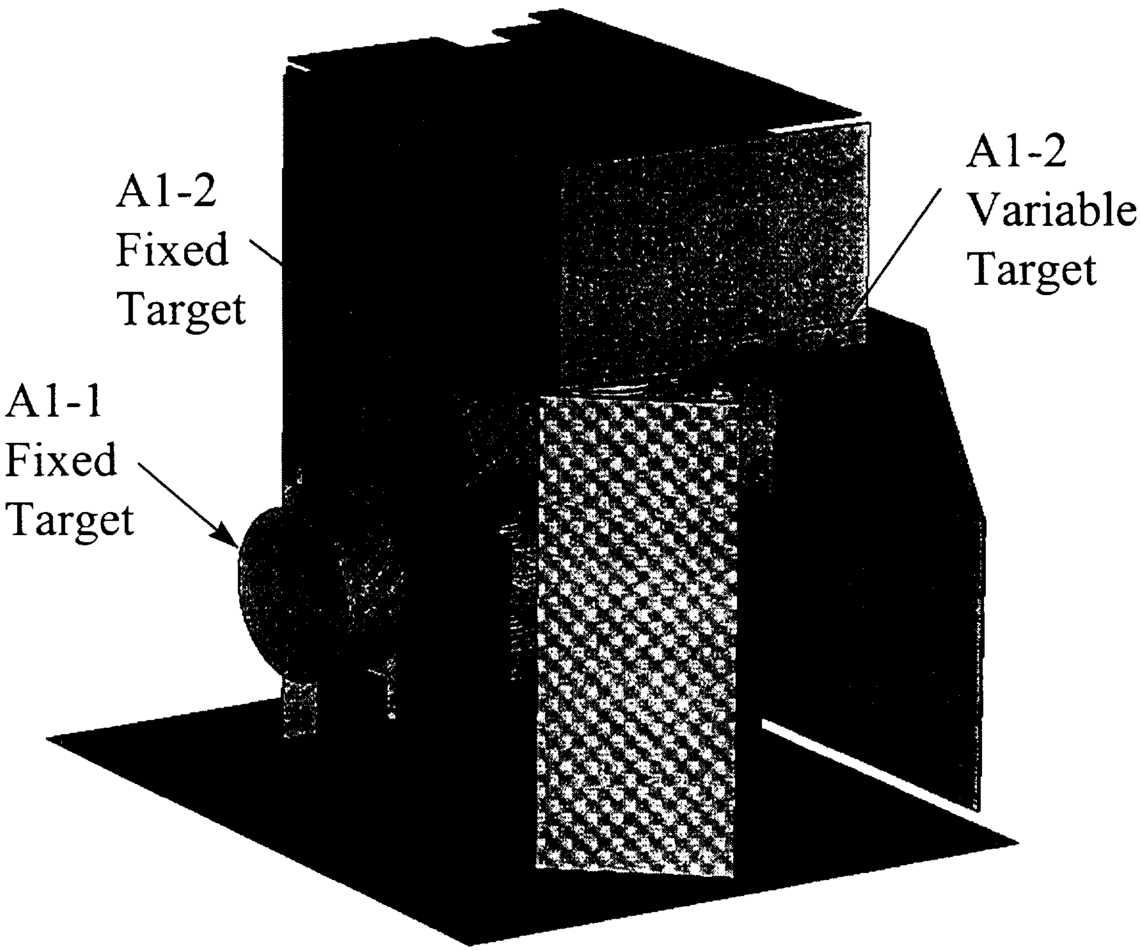

Figure 1. Geometric thermal model eosa1dcq.inp.
Complete model with targets.

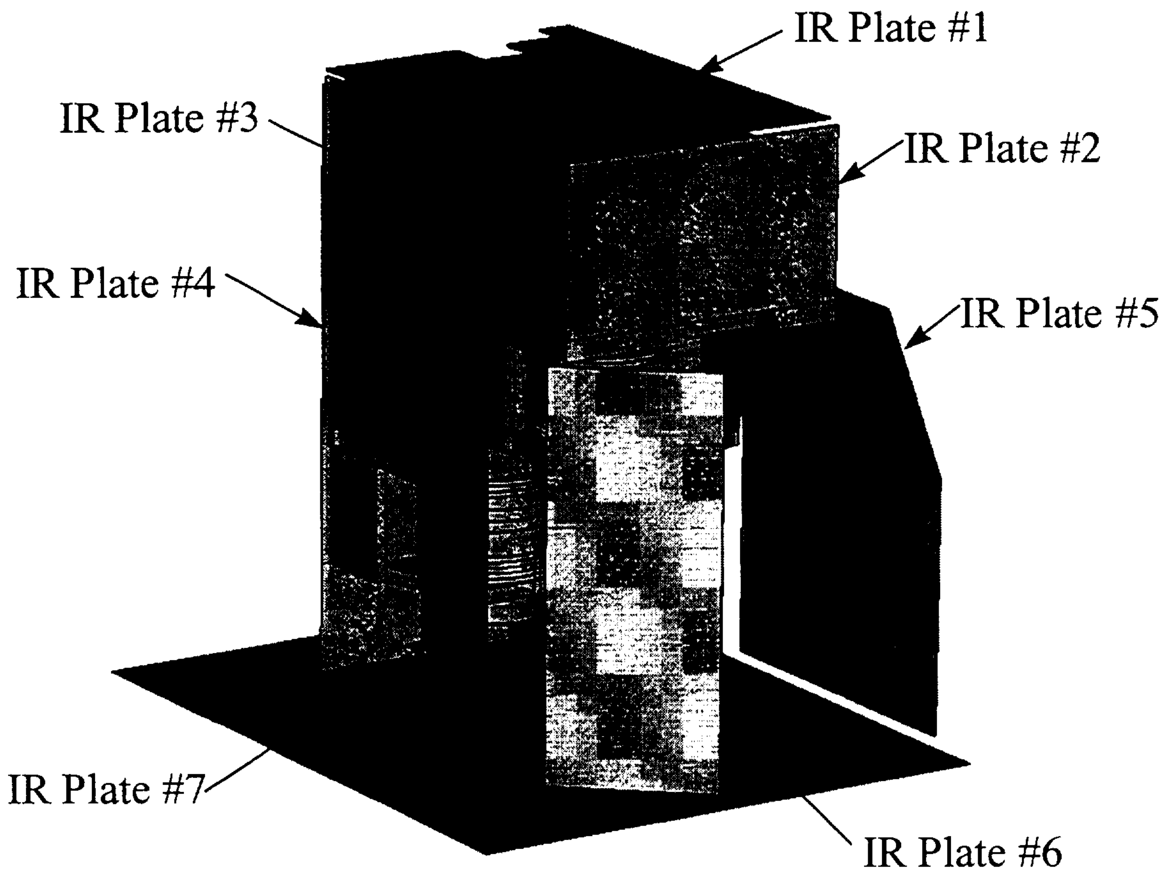

Figure 2. Geometric model eosa1dcq.inp.
Targets removed, IR Plates identified.

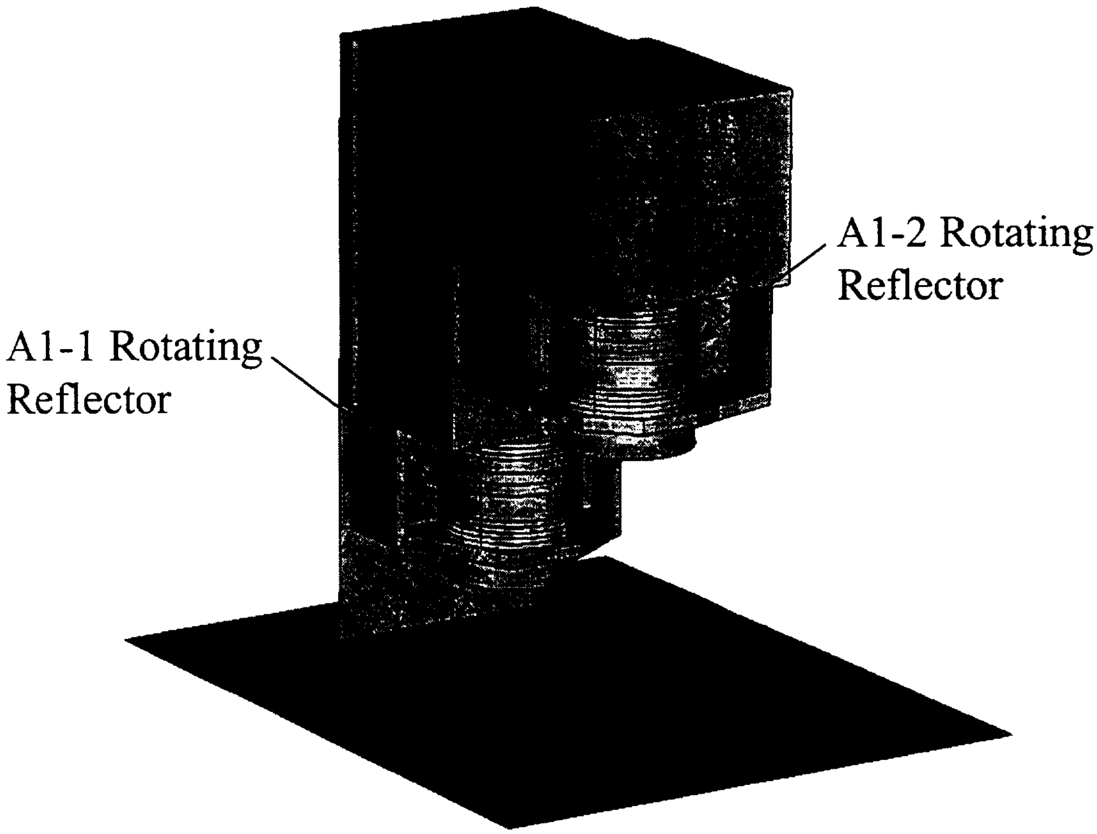

Figure 3. Geometric model eosa1dcq.inp.
IR plates removed, reflectors identified.

DOCUMENT APPROVAL SHEET

GENCORP AEROJET

TITLE			DOCUMENT NO.
Engineering Test Report AMSU EOS A1 Thermal Balance Test Correlation			Report 11340 11 November 1998
INPUT FROM: DATE R. J. Krylo	CDRL: 207	SPECIFICATION ENGINEER: DATE N/A	
CHECKED BY: DATE N/A		JOB NUMBER: DATE N/A	

APPROVED SIGNATURES	DEPT. NO.	DATE
Product Team Leader (L. Paliwoda) Lucy Paliwoda	7888	11-18-98
Systems Engineer (R. Platt) R W Platt	8341	11/19/98
Design Assurance (E. Lorenz) E. Lorenz	8331	11/18/98
Quality Assurance (R. Taylor) RM Taylor	7831	11-18-98
Technical Director/PMO (R. Hauerwaas) RV Hauerwaas	4001	11/19/98
Released: Configuration Management (J. Cavanaugh) J Cavanaugh	8361	11/19/98

By my signature, I certify the above document has been reviewed by me and concurs with the technical requirements related to my area of responsibility.

(Data Center) FINAL

Please return this sheet and the reproducible master to Jim Kirk (Bldg. 1/Dept. 8631), ext. 2081.